Q. J. R. Meteorol. Soc. (2002), **128**, pp. 1293–1319

The cold Arctic winter 1995/96 as observed by GOME and HALOE: Tropospheric wave activity and chemical ozone loss

By M. WEBER[1]*, K.-U. EICHMANN[1], F. WITTROCK[1], K. BRAMSTEDT[1], L. HILD[1], A. RICHTER[1], J. P. BURROWS[1] and R. MÜLLER[2]

[1]*University of Bremen FB1,Germany*

[2]*Forschungszentrum Jülich ICG-1, Germany*

(Received 29 January 2001; revised 15 August 2001)

SUMMARY

The Global Ozone Monitoring Experiment aboard the European Remote Sensing Satellite ERS-2 was the only satellite instrument measuring total ozone on a near-global scale during the extremely cold Arctic winter 1995/96. Extremely low total ozone was observed within the Arctic vortex during February and March. The lowest value in this winter was 178 DU (Dobson units) over Greenland on 19 February, which was about 160 DU below the February Arctic vortex mean of total ozone. Although severe chemical ozone destruction occurred in late winter 1995/96, the extremely low values in total ozone observed after the middle of February were, in all cases, related to mini-hole events, where large horizontal divergent transport of ozone from the lower-stratospheric layer above a high tropopause rapidly reduced the total column in a localized region. The observed total-ozone minima were located near the vortex edge and in the region of minimum lower-stratospheric temperatures that were, in selected cases, sufficiently low for the formation of polar stratospheric ice clouds (PSC type II) below 188 K at the isentropic level of 475 K. Coincident ozone profile observations in early March from the Halogen Occultation Experiment on the Upper Atmosphere Research Satellite indicate that the strong chemical ozone loss was mainly confined to the polar vortex region, and that the extremely low total-ozone values below 250 DU were mainly caused by short-term reversible dynamical reductions superimposed upon chemical ozone loss occurring on longer timescales. Enhanced OClO and chlorine activation, due to strong tropospheric wave activity associated with an ozone mini-hole event, was only observed in early March following a stratospheric temperature drop below the ice frost point. In general, however, the observation of very low total ozone in mini-hole events does not necessarily point to significant additional chemical depletion.

KEYWORDS: Mini-holes Polar meteorology Satellite observations Stratosphere

1. INTRODUCTION

Heterogeneous reactions on polar stratospheric cloud (PSC) surfaces that form at low temperatures in the polar winter regions of the stratosphere convert chlorine containing reservoir compounds into photochemically active species. The latter cause rapid catalytic chemical destruction of stratospheric ozone when sunlight returns to the polar regions during spring (Solomon *et al.* 1986; Solomon 1999). Since the middle of the 1980s large springtime ozone depletion has been regularly observed in the polar vortex above Antarctica (e.g. Cubashi 1984; Farman *et al.* 1985; Herman *et al.* 1993; Manney *et al.* 1993; Waters *et al.* 1993). Despite the hemispheric difference in ozone distribution, i.e. greater winter/spring ozone maxima, larger natural variability in ozone, and higher stratospheric temperatures in the northern hemispheric winters, substantial chemical ozone losses, mainly confined to the lower stratosphere, were unequivocally identified in the Arctic vortex from recent ground-based and ozone-sonde data (Braathen *et al.* 1994; Larsen *et al.* 1994; Donovan *et al.* 1995, 1996, 1997; von der Gathen *et al.* 1995; Rex *et al.* 1997, 1998; Knudsen *et al.* 1998; Sinnhuber *et al.* 1998), airborne observations (Proffitt *et al.* 1990), and satellite measurements (Manney *et al.* 1994, 1995, 1996a, 1996b, 1997; Müller *et al.* 1996, 1997a, 1997b, 1999). The first observational evidence for chemical ozone depletion in the Arctic was obtained in 1988/89 and subsequent winters (Hofmann *et al.* 1989; Proffitt *et al.* 1990; Schoeberl *et al.* 1990).

* Corresponding author: Institute of Environmental Physics, University of Bremen FB1, PO Box 330 440, D-28334 Bremen, Germany. e-mail: mark.weber@iup.physik.uni-bremen.de

The Arctic winter/spring season 1995/1996 was one of the coldest winters on record; temperatures were sufficiently low for the existence of PSCs on a maximum number of days, based upon the 30-year record of stratospheric temperatures at 30 hPa and 50 hPa from the Free University of Berlin data (Naujokat and Pawson 1996) (see also Fig. 6 in the paper by Pawson and Naujokat (1997) and Fig. 2 in the paper by Pawson and Naujokat (1999)). The Arctic winter of 1995/96 has attracted much attention because it was a winter with severe accumulated chemical ozone depletion observed inside the vortex (Manney *et al.* 1996a; Donovan *et al.* 1996). From ozone-sonde measurements, a chemical loss of 64% was deduced by Rex *et al.* (1997) in the stratospheric layer bounded by the 470 K isentropic surface (a height of 19–20 km) by the end of March and, from the Halogen Occultation Experiment (HALOE), an accumulated chemical loss of about one third was found (Müller *et al.* 1997a) in the column amount between the 350 and 550 K isentropic surfaces (12–21 km) by early April. It is well known that variations in total ozone are also caused by transport related to wave activity (Petzoldt *et al.* 1994; Orsolini *et al.* 1998; Chipperfield and Jones 1999). The important role of tropospheric wave activity, in addition to strong chemical depletion, on observed Arctic ozone evolution during the winter of 1995/96 is investigated here in greater detail, based on observations from the Global Ozone Monitoring Experiment (GOME) and HALOE in combination with meteorological data.

GOME aboard the ERS*-2 was the only total-ozone measuring satellite instrument with high spatial resolution and near-global coverage operating during the winter/spring of 1995/96. It provides, therefore, a unique opportunity to obtain a synoptic view of this period. 1995/96 was also the first complete northern hemisphere (NH) winter/spring season to be covered by GOME following its launch in April 1995 (Burrows *et al.* 1999). This paper provides an overview of the Arctic winter 1995/96 based upon trace-gas observations from GOME and HALOE, together with analyses from the ECMWF† and MO‡ meteorological datasets. The focus in this paper is on the strong tropospheric wave activity near the polar vortex edge during February and early March, which led to a record number of so-called days of possible PSC II occurrences (temperatures below 188 K at the 475 K isentropic level), particularly in late winter. A question that arises is: what might the contribution of enhanced tropospheric wave activity have been to the accumulated chemical ozone observed inside the vortex over the course of the winter? After a brief description of the GOME and HALOE data analyses (sections 2 and 3), the meteorology and the evolution of the Arctic vortex monthly-mean total ozone between November 1995 and April 1996 are presented. In order to highlight the peculiarity of that winter, a brief comparison is made with observations by GOME during the subsequent winters between 1996/97 and 1999/2000 (section 4). The development of ozone mini-hole events in association with upper-tropospheric wave activity near the Arctic vortex edge are investigated by comparing GOME observations with potential-vorticity (PV) maps derived from the MO meteorological dataset. Clear indication of enhanced dynamically induced PSC formation and subsequent chlorine activation are supported by GOME OClO observations after the ozone mini-hole event in early March (section 5). On the other hand, when the available active chlorine (Cl_y) was already fully activated, as was apparently the case in mid February, no additional enhancement of active chlorine and OClO was observed following a strong stratospheric cooling due to subtropical-air intrusion. From collocated GOME and HALOE observations in early

* European Remote Sensing satellite.

† European Centre for Medium-Range Weather Forecasts.

‡ Met Office.

March 1996 (Müller *et al.* 1997a, 1999), the chemical ozone losses inside the vortex have been quantified, while in the region of lowest total ozone the contribution of chemical depletion was either small or negligible at the vortex edge and outside the vortex, respectively (section 6).

2. Instruments and data analysis

(*a*) *GOME*

The GOME ultraviolet/visible spectrometer aboard ERS-2 has a double monochromator design and covers the entire spectrum from 240 to 790 nm at a spectral resolution varying between 0.2 and 0.3 nm in four separate spectral channels (Weber *et al.* 1998; Burrows *et al.* 1999). ERS-2 was launched into a sun-synchronous near-polar orbit at a mean altitude of 795 km. The equator crossing time in the descending node is at 1030 h local time. GOME is a nadir-viewing instrument and its measurement sequence consists of an across-track scan cycle lasting 4.5 s, three radiance measurements in the forward direction each covering a maximum surface area of 40 km along-track by 320 km across-track, and a back scan. Employing the maximum scan width of 960 km across-track, global coverage is achieved after 42 orbits, or approximately three days. At latitudes higher than 65° complete coverage, except for the polar night region, is provided each day.

The total-ozone data presented here are contained in Version 2.70 of the GOME Data Processor (GDP). By comparing GDP Version 2.40 data with collocated ground-based measurements from the Network for the Detection of Stratospheric Change (NDSC) a global agreement to within ±4% was found (Lambert *et al.* 1999a). At high solar zenith angles (>75°) larger differences of up to ±10% have been found. In the polar region, GOME overestimates the lowest columns (<260 DU*) and underestimates the highest columns by an average of 4%. The best agreement is observed around 300 DU (Lambert *et al.* 1999a). A similar conclusion can be drawn from the comparison with the Version 2.70 data, implying that the accuracy of total ozone derived from GOME did not change significantly between Versions 2.40 and 2.70 (Lambert *et al.* 1999b). The agreement between TOMS† and GOME inside the polar region (63°–90°N) is better than 1.5%. The GOME March 1996 value of 369 DU north of 63°N is about 2% smaller than the 377 DU derived from the Solar Backscatter Experiment (SBUV/2) aboard the NOAA-9 satellite (Newman *et al.* 1997).

GOME level-1 spectra have been analysed using the differential optical absorption (DOAS) algorithm to derive slant columns of NO_2 and OClO (Wittrock *et al.* 1999; Richter *et al.* 1998; Burrows *et al.* 1999). For the NO_2 data presented below, the fitting has been restricted to the spectral region 425–450 nm, similar to that used for ground-based measurements. In the case of OClO, the fitting region 357.0–381.5 nm has been selected. An extraterrestrial solar spectrum measured by GOME was taken as a background spectrum in the DOAS retrieval. Assuming that OClO is completely photolysed under sunlit conditions, the residual slant column retrieved near the equator (most likely due to some instrumental artefact) has been subtracted from all results within a GOME orbit. Slant columns have been converted to vertical columns using air-mass factors (AMFs) computed with a multiple-scattering radiative-transfer model GOMETRAN (Rozanov *et al.* 1997) assuming simple standard profiles for NO_2 and OClO. Chemical enhancement of AMFs, as well as the seasonal variation of the

* Dobson Units.

† Total Ozone Monitoring Satellite.

atmospheric constituents, have been neglected. The absolute errors in the NO_2 and OClO vertical columns are conservatively estimated at 20% and 50%, respectively. The largest uncertainty stems from the AMF calculation. This is particularly true for OClO because of its rapid photolysis after sunrise.

(*b*) *HALOE*

The HALOE instrument aboard the Upper Atmosphere Research Satellite (UARS) measures O_3, H_2O, NO_2, NO, HCl, HF, and CH_4 by solar occultation (Russell *et al.* 1993). Fifteen sunrise and sunset measurements are normally performed each day along two approximately constant latitude belts that move between 80°S and 80°N in about 45 days. Arctic vortex observations were possible in January, March and April 1996. Early polar vortex air was observed in November 1995, which made it possible to derive a relation between ozone and methane that yields a proxy for the ozone expected in absence of chemical depletion (Müller *et al.* 1996, 1997a, 1999).

The vertical resolution of the HALOE observations is approximately 2 km for ozone and 4 km for CH_4. For ozone data below 25 km the root-mean-squares error is about 15% for low stratospheric aerosol loadings (as it was the case in winter 1995/96) and above (up to 60 km) of the order of 5%; the error bars for methane are about ±10% below 50 km. Agreement with correlative measurements is within 5–10% and about 15% throughout the stratosphere for O_3 and CH_4, respectively, based upon Version-17 HALOE data (Brühl *et al.* 1996; Park *et al.* 1996). Here, as in earlier studies on this winter (Müller *et al.* 1997a, 1999), we use Version-18 HALOE data, with an improved data quality. For ozone, this improved quality of Version-18 ozone data has been demonstrated through intercomparison of HALOE measurements with those from SAGE* II and from ozone sondes (Liu *et al.* 1997).

3. Polar meteorology and GOME total ozone in 1995/96

(*a*) *Polar vortex evolution and PSC formation*

PSC particles form in the lower stratosphere at sufficiently low temperatures. Solid (PSC type Ia) and liquid (PSC type Ib) particles, consisting of HNO_3 and H_2O, occur at temperatures below approximately 195 K, and ice particles (PSC type II) form if temperatures fall below approximately 188 K. The last type is the most efficient for heterogenous chlorine activation. The exact temperatures for these phase transitions depend on altitude and on the HNO_3 and H_2O partial pressures (Peter 1997). The number of days with temperatures below those needed for PSC type I and II existence at 50 hPa during the four most recent winters are summarized in Table 1. It can be concluded that the Arctic winter 1995/96 was an extremely cold winter with a record number of days below the PSC I existence temperature (98 days below 195 K) and below the PSC II frost point (24 days below 188 K). This record still holds if one includes the 30-year statistics (1966–1996), as shown in Fig. 6 of Pawson and Naujokat (1997). Particularly striking is the fact that, for none of the recent cold winter/spring seasons (e.g. 1996/97 and 1999/2000), temperatures below 188 K were observed in February according to the Free University of Berlin analyses (see Table 1). Combined dehydration (ice-particle sedimentation) and denitrification in well defined layers have been observed in January and February 1996 (Vömel *et al.* 1997; Hintsa *et al.* 1998). Dehydration is normally a rather rare event in the NH, as opposed to the Antarctic where the lower-stratospheric temperatures are persistently lower than in the NH.

* Stratospheric Aerosol and Gas Experiment.

TABLE 1. NUMBER OF DAYS WHEN THE MINIMUM TEMPERATURE AT 50 hPa WAS BELOW THE TEMPERATURE FOR POSSIBLE PSC TYPE I (195 K) AND TYPE II (188 K—FIGURES IN BRACKETS) EQUILIBRIUM EXISTENCE

Year	Total	November	December	January	February	March
1995/96	98(24)	1	31	31(9)	28(13)	7(2)
1996/97	84(0)			26	28	30
1997/98	51(0)	1	21	13	15	1
1998/99	18(0)	1	9		8	
1999/00	94(7)		24	31(7)	29	10

Data obtained from the Free University of Berlin analyses (Pawson and Naujokat 1999; B. Naujokat, personal communication).

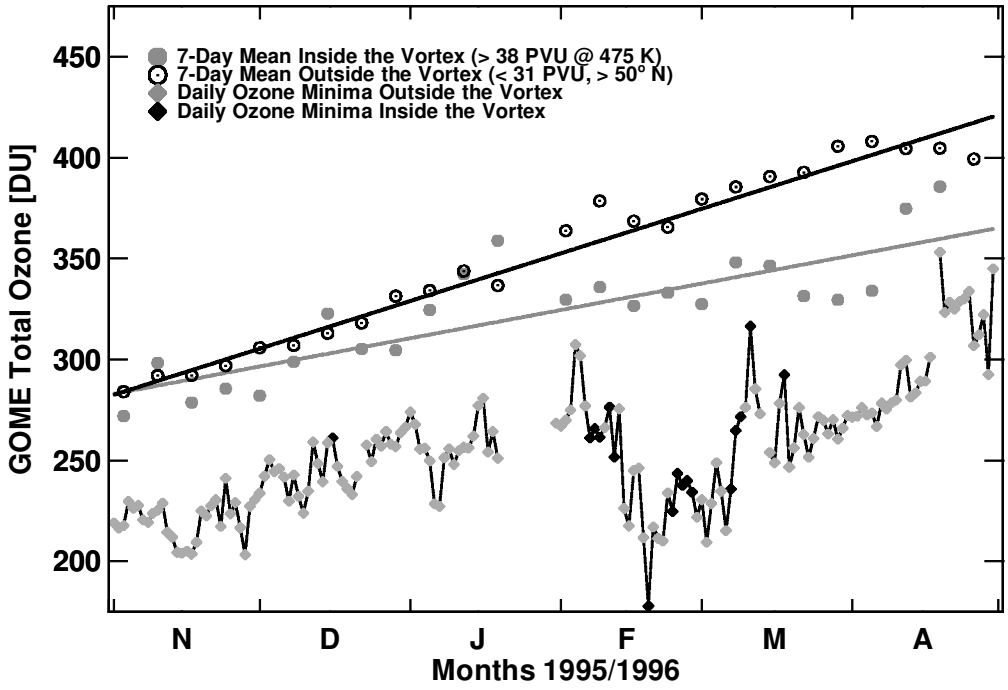

Figure 1. Time series of weekly GOME total ozone in the northern hemisphere during the winter/spring of 1995/96. Solid circles show the weekly-mean values in the inner part of the Arctic vortex (potential vorticity greater than 38 PVU at the 475 K isentropic level in the European Centre for Medium-Range Forecasts analyses), and open circles show the weekly-mean total ozone north of 55°N outside the polar vortex (potential vorticity less than 31 PVU at the 475 K isentropic level). In the second half of January, and for a few days in March, no data were available from GOME. The diamonds indicate the daily minimum total ozone observed in the northern hemisphere (the black diamonds indicate the minimum values observed inside the polar vortex). The record low value of 178 DU was observed at the southern tip of Greenland on 19 February 1996.

(*b*) *GOME Arctic total-ozone observations*

Figure 1 shows a time series of weekly-averaged total ozone inside the vortex, as observed by GOME during the winter/spring 1995/96, in comparison with mean values outside the vortex. The vortex area is defined by the region with PV values higher than 38 PVU* at the 475 K isentropic level (38 PVU@475K). The vortex edge region is located between 31 and 44 PVU (see the appendix for the vortex boundary definition). One should note here, that the Arctic vortex-mean values in early winter

* Potential vorticity unit: 1 PVU $= 1\times10^{-6}$ K m^{2}kg^{-1}s^{-1}.

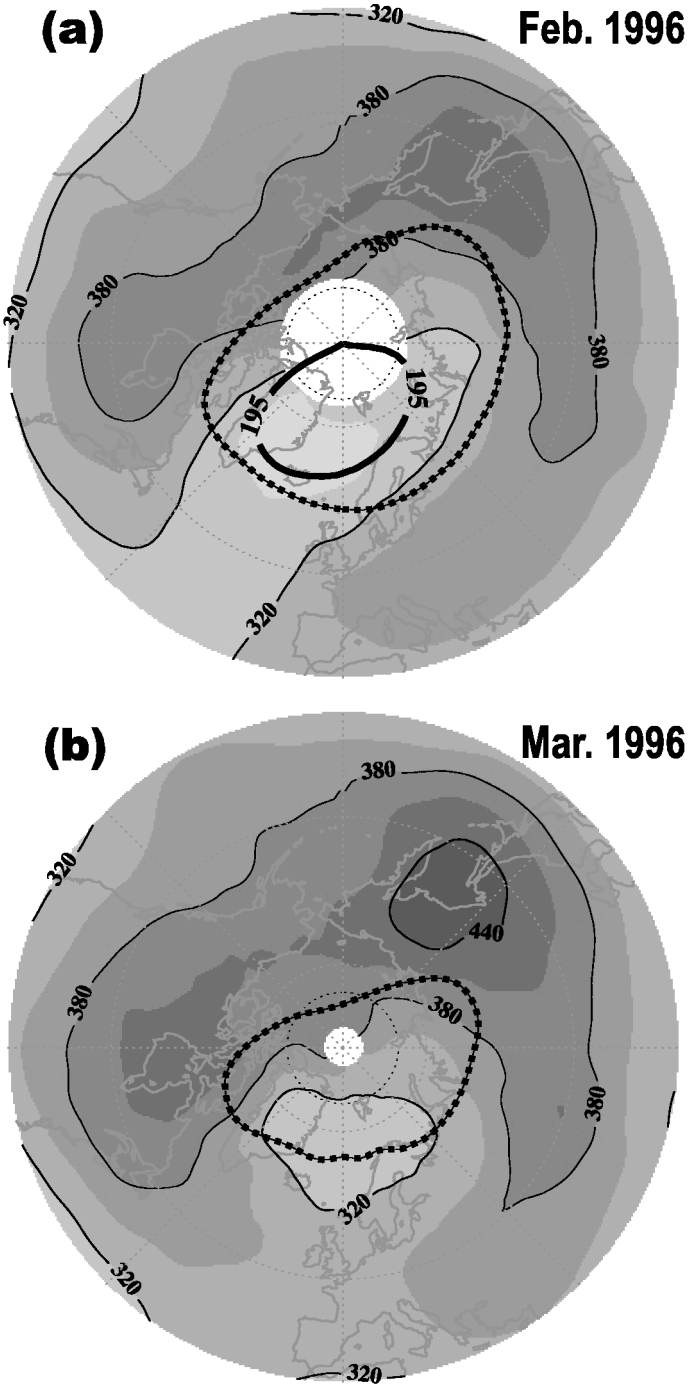

Figure 2. GOME northern hemisphere total-ozone distribution. The monthly-mean position of the polar vortex edge is indicated by the 38 PVU potential-vorticity contour at the 475 K isentropic level (heavy dotted line) and the thick solid line shows the area where the temperature at the same altitude was, on average, below the PSC I formation temperature of 195 K (according to the European Centre for Medium-Range Forecasts analyses). The maps are stereographic projections with the Greenwich meridian at the bottom and the outer circle at 35°N.

TABLE 2. MEAN TOTAL OZONE (DU) IN THE ARCTIC VORTEX

Year	February	March	April
1996	332	337	358
1997	362	351	361
1998	365	393	438
1999	422	481	*
2000	364	361	389

* Sample too small or zero.
The Arctic vortex is defined as the region with potential vorticity larger than 38 PVU at the 475 K isentropic level.

are not considered reliable because extended regions of the Arctic were inside the polar night, and so the sampling of the vortex by GOME was limited. The third curve indicates the daily total-ozone minimum values at 55°N and higher. Starting in early February the NH ozone minimum dropped significantly by about 50 DU. These events were located at the vortex edge. In February and March the vortex-mean values were about 40 DU below the mean value outside the polar vortex. Until the middle of March this difference did not seem to increase significantly despite the onset of the enhanced tropospheric wave activity and the decrease of observed daily ozone minima (see Fig. 1).

Figure 2 shows the monthly-mean NH total-ozone distribution in February and March. Monthly-mean vortex ozone amounts of 332 DU and 337 DU were observed by GOME in February and March 1996, respectively (Table 2). Typical long-term climatological values for March from the Dobson station at Tromsø (69.4°N) are 440 ± 50 DU (Hansen *et al.* 1997) and the March average over the polar region (from 63°N to 90°N) from SBUV* radiation and Nimbus 7 total-ozone measurements from late 1970s and the 1980s was about 445 DU (Newman *et al.* 1997), which is about 110 DU higher than observed in March 1996. Again, extremely low ozone is observed near or just inside the vortex edge in the North Atlantic sector as a consequence of the strong mini-hole formation associated with tropospheric wave activity.

(*c*) *Comparison of GOME observations with later winter/spring seasons*

To put the winter/spring season of 1995/96 into a better perspective we examine the GOME observations of the subsequent winters between 1996/97 and 1999/2000. In 1996/97, the Arctic vortex started to form comparatively late in December and record low temperatures in the lower stratosphere were observed at the end of March (Coy *et al.* 1997). The vortex break-up, in terms of maximum westerly wind speeds reducing to below 15 m s^{-1}, was also delayed towards the second half of April, about a month later than in the season before. The subsequent winters, 1997/98 and 1998/99, exhibited minimum lower-stratospheric temperatures in the Arctic that were higher than in the two seasons before. The winter 1997/1998 minimum lower-stratospheric temperatures were close to the long-term mean, while the winter 1998/99 exhibited minimum lower-stratospheric temperatures that were well above the long-term means in December and early January, and were associated with the first major stratospheric warming observed in nearly eight years (Manney *et al.* 1999). In 1998 and 1999 the March values increased to 403 DU and 490 DU, respectively (see Table 2). The most recent winter/spring season, 1999/2000, matched again the series of cold Arctic winters in the 1990s, with 94 days with temperatures below possible PSC I formation (<195 K at the 475 K isentropic

* Solar Back-scattered UltraViolet.

level). However, no days with temperatures below the frost point of PSC II type clouds were observed after the end of January in 2000.

The vortex-mean total-ozone amounts inside the Arctic vortex in March 1996, 1997, and 2000 (337 DU, 351 DU, and 364 DU, respectively) were at a record low in comparison with satellite measurements available since 1979 (Newman *et al.* 1997). A major distinction between the cold winters in 1995/96 and 1996/97, apart from the long persistence of the polar vortex in spring 1997, was the difference in the level of tropospheric wave activity, which was intense in late winter 1995/96 (see section 4) but weak in 1996/97 (Coy *et al.* 1997). This might be the reason why both the February and March monthly vortex-mean ozone amounts in 1996 were the lowest in the GOME data record. The last five Arctic winters clearly document the large interannual variability of the meteorology and total ozone in the Arctic.

(*d*) *Sequences of daily total-ozone distribution in February and March 1996*

Figures 3 and 4 show daily total-ozone maps of the NH on selected days in February and March 1996, respectively. On 10 February 1996 (Fig. 3(a)) the total-ozone values were reduced to between 275 and 350 DU inside the Arctic vortex, which was elongated from the North Atlantic to eastern Siberia. Five days later, a cold region with lower-stratospheric temperatures below 188 K and observed total-ozone amounts well below 250 DU developed just outside the vortex (Fig. 3(b)). The lowest total ozone at polar latitudes in late winter 1995/96, with a value of 178 DU, was observed on 19 February above Greenland (Fig. 3(c)). The omega-shaped vortex boundary in the vicinity of the ozone minimum is related to polar intrusion of upper-tropospheric subtropical air raising the tropopause below the base of the polar vortex (Manney *et al.* 1996a; O'Neill *et al.* 1994). This event reduced the lower-stratospheric temperatures to allow possible PSC type II occurrence at the 475 K isentropic level. This mini-hole moved eastward along with the cold centre crossing the North Atlantic and reaching Scandinavia two days later (21 February, Fig. 3(e)). On 22 February the mini-hole appeared to have moved inside the polar vortex near the Barents Sea (Fig. 3(f)). As is shown in section 4, the mini-hole coincided with a cut-off anticyclone stemming from the tropospheric ridge formed earlier.

Another mini-hole sequence is observed during the first days of March (see Fig. 4). On 6 March 1996 the stratospheric temperatures at the 475 K isentropic level were below the possible PSC equilibrium existence temperature (195 K) for the last time during that winter/spring season, according to the ECMWF meteorological analysis (Fig. 4(d)). On 8 March 1996 the vortex boundary on the 475 K isentropic surface is strongly distorted, reaching 80°N north of Scandinavia, forcing a northward excursion of the polar jet stream along the PV isolines (Fig. 4(e)). Low total ozone inside the vortex was still observed throughout March when the final warming continued (Fig. 4(f)).

The ozone distribution on 3 March 1996 depicted in Fig. 4(b) shows that low total-ozone values occur within the confines of the polar vortex, but it clearly extends outside the vortex region as well. This finding is consistent with Microwave Limb Sounder (MLS) observations which show that, although the region of low ozone mixing ratios in the lower stratosphere (approximately at the height of the 465 K isentropic surface) in early March 1996 is well situated inside the polar vortex, the column amounts above 100 hPa correlate more closely with the minimum-temperature region that also extrudes outside of the vortex region (Manney *et al.* 1996a). Both Figs. 2 and 3 clearly show that the region of minimum total ozone correlates better with the region of minimum lower-stratospheric temperature than with the polar vortex area, showing the strong linkage

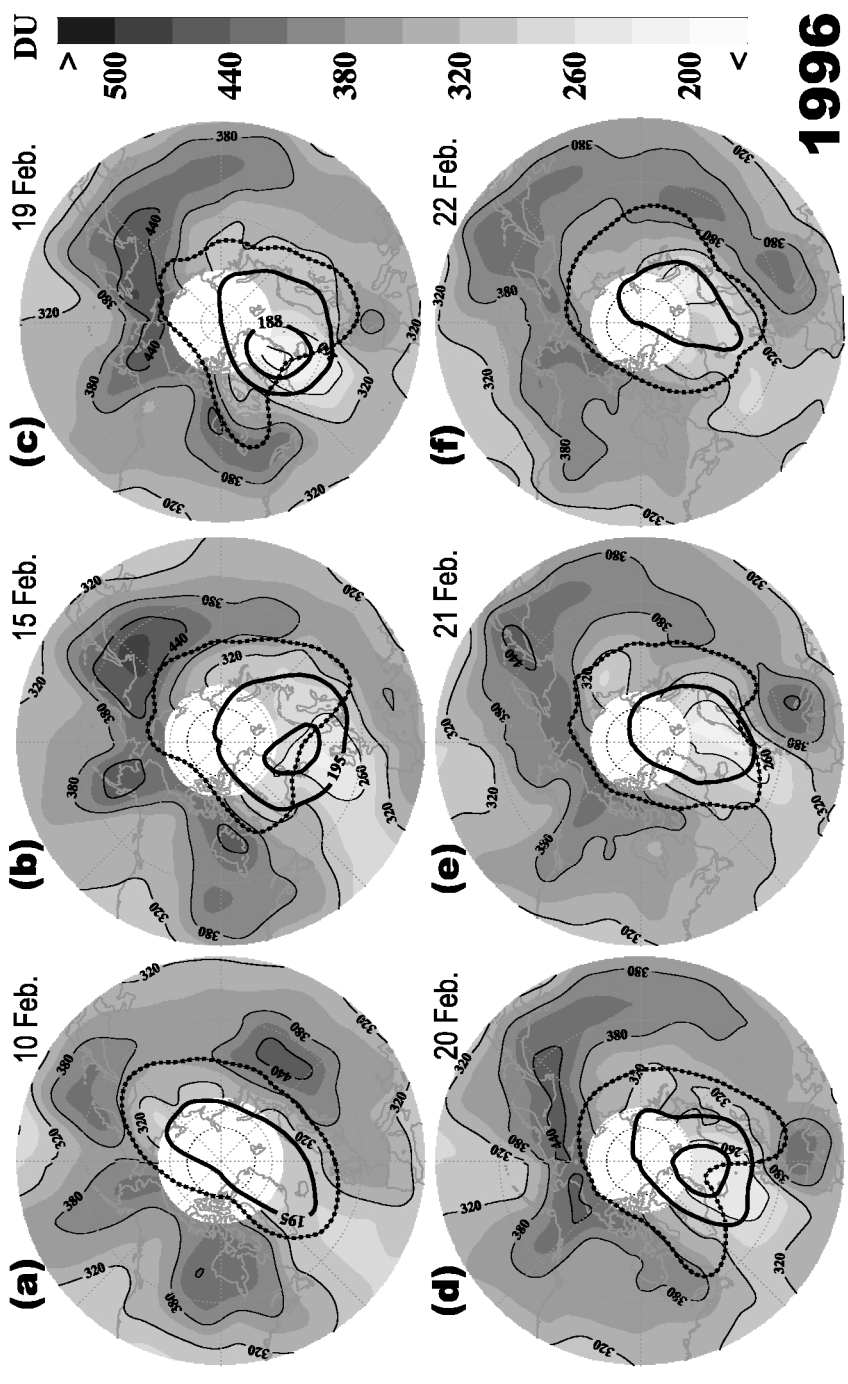

Figure 3. GOME February northern hemisphere total-ozone distribution for selected dates: 10, 15, 19, 20, 21, and 22 February 1996. The maps are stereographic projections with the Greenwich meridian at the bottom and the outer circle at 35° N. Isolines of potential vorticity equal to 38 PVU at the 475 K isentropic level (according to European Centre for Medium-Range Forecasts analyses) are shown as heavy dotted lines. Lower-stratospheric temperature contours of 188 K and 195 K at the 475 K isentropic level are indicated by thick solid lines (with the 188 K contour inside the 195 K one if the PSC II formation temperature is reached). Gridding of the daily GOME data was done by binning the average of the three closest-neighbour values within an 800 km distance into a $1.25° \times 1°$ longitude–latitude grid. Data gaps have been filled with spline-interpolated values in the longitudinal direction and the ozone field was finally smoothed by convolving the data with a five-point-wide two-dimensional triangular function.

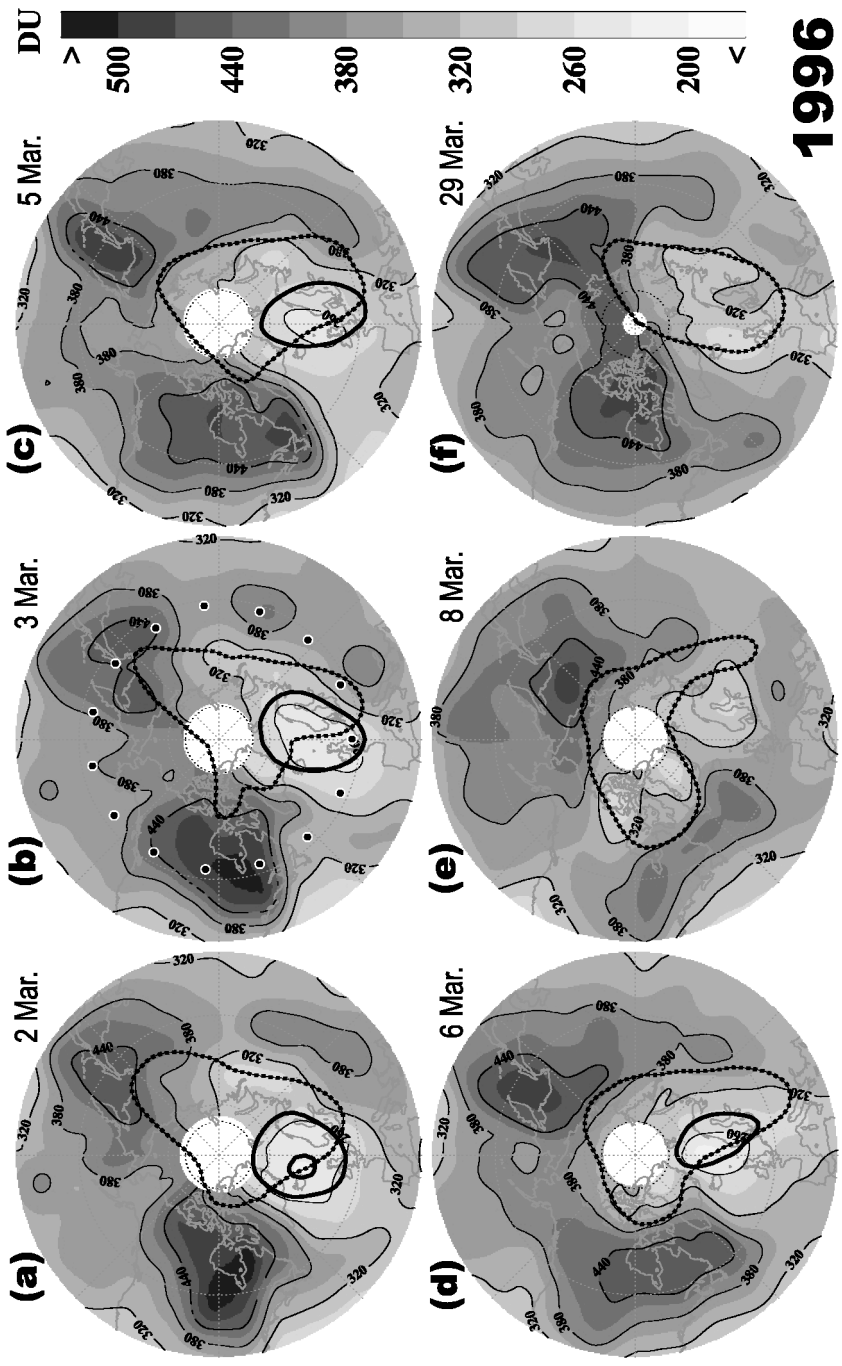

Figure 4. As Fig. 3, but for the selected dates: 2, 3, 5, 6, 8, and 29 March 1996. HALOE measurement points on the 52°N latitude circle on 3 March 1996 are also shown in (b) (see section 6).

between tropospheric wave activity, the lower-stratospheric temperatures, and the total ozone (Petzoldt *et al.* 1994).

HALOE measurements of vertical ozone profiles show very low mixing ratios inside the polar vortex in March and early April 1996 (Müller *et al.* 1997a, 1999). These observations are in accordance with the notion that substantial chemical ozone loss occurred inside the Arctic vortex. Combining the HALOE and GOME observations, the contribution of chemical loss to the overall reduction in total-ozone column is investigated in more detail in section 5.

4. Meteorology and chemistry of the late-winter ozone mini-holes

(*a*) *Tropospheric wave activity*

The development of the mini-hole sequence as shown in Figs. 3 and 4 is examined more closely by looking at the PV on the 325 K isentropic surface, which is near the tropopause region. The analysis presented here is based upon the MO meteorological dataset available in a $3.75^\circ \times 2.5^\circ$ (longitude–latitude) grid resolution (Swinbank and O'Neill 1994). In Fig. 5 the evolution of the tropopause with time during the period from 18 to 22 February is visualized by the shaded contour representing the 3–4 PVU range. A value of 3.5 PVU provides a good estimate of the dynamical tropopause outside the tropics (Hoerling *et al.* 1991). This PV contour separates subtropical air from the polar air masses i.e. polewards of the shaded area the PV increases and the tropopause height decreases to lower isentropic levels, while equatorwards the opposite takes place. In a frictionless and adiabatic air-mass flow, PV is conserved (Hoskins *et al.* 1985) and, therefore, the evolution of the PV contour with time permits the study of the upper-tropospheric and lower-stratospheric Rossby wave propagation (Peters and Waugh 1996).

Poleward advection of subtropical air masses occurred above the southern tip of Greenland on 18 February (Fig. 5(a)). The tongue of low PV air then propagated eastward and reached almost 80°N (south of Spitsbergen) during the following two days. Its tip extended well into the polar vortex region, as indicated by the 475 K vortex boundary overlaying the PV contour on the 325 K isentropic surface. Just inside the vortex a cold centre, with temperatures below 188 K at the 475 K isentropic level, formed and followed the tropospheric ridge for about four days, after which the temperature started to increase to values above 195 K (Figs. 5(a)–(d)). After the ridge and the cold centre crossed Scandinavia, the anticyclone became cut off from the tongue when it reached the Siberian Sea on 22 February (Fig. 5(e)). On that day the 3.5 PVU surface inside the anticyclone peaked at a geopotential height of more than 14 km, which corresponds to a tropopause lifting in the range of 4 to 6 km at polar latitudes. The poleward shifting of the stratospheric jet stream around the tropospheric ridge is also clearly seen in the PV contour sequence shown in Fig. 5. Minimum total-ozone values inside the anticyclone remained below 250 DU for about six days and followed the motion of the tropospheric ridge (Fig. 2).

(*b*) *Trace-gas observations: Ozone, NO_2, OClO, and methane*

Figure 6 depicts the NO_2 vertical-column distribution in the NH, as measured by GOME on 19 February 1996. Very low NO_2 levels (below 2×10^{15} molecules cm^{-2}) are detected inside the vortex above Greenland and north of Iceland. In this region depleted gas-phase nitric acid (HNO_3) was observed by the MLS in the lowermost stratosphere, which confirms the phase transitions of HNO_3 into solid or liquid particles

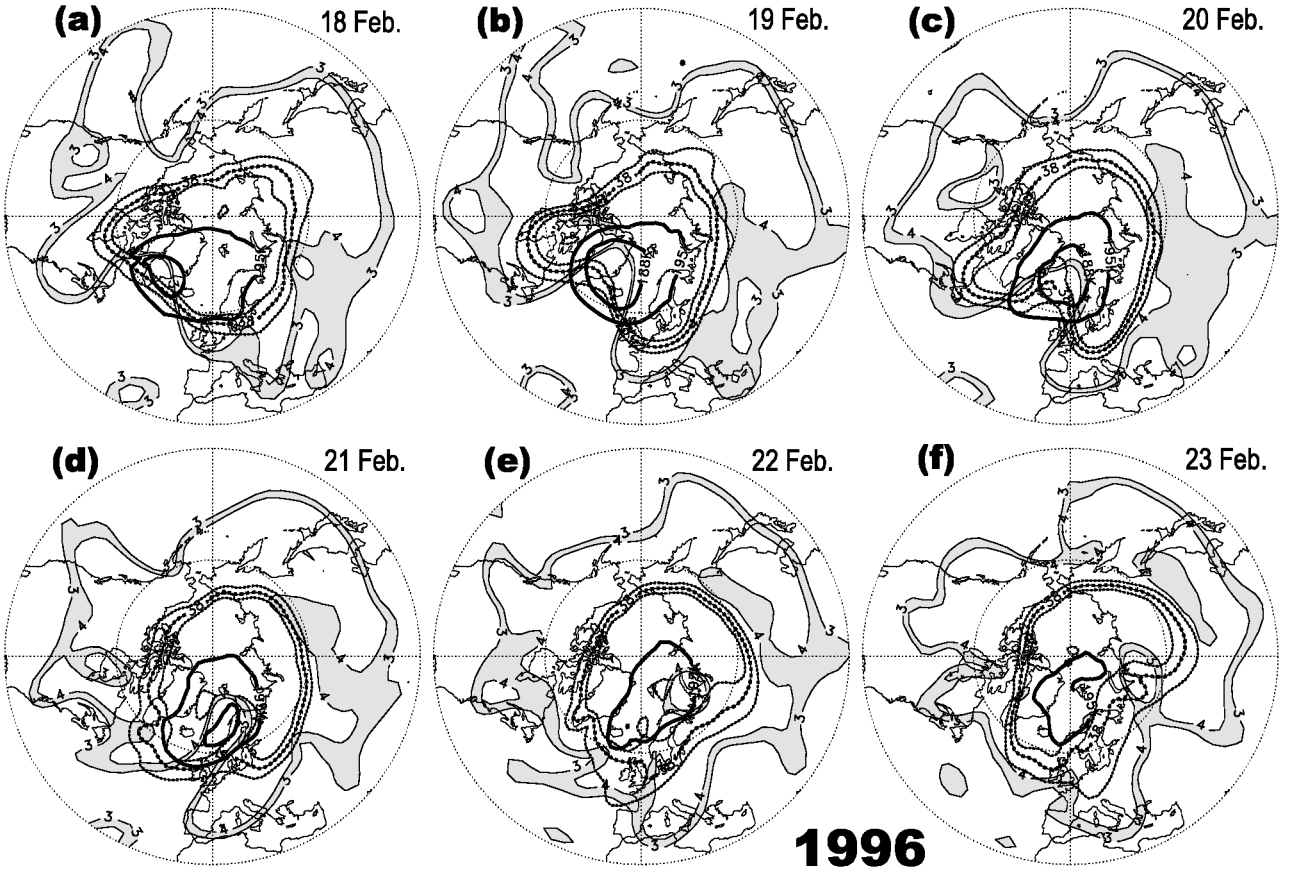

Figure 5. Rossby wave breaking in the upper troposphere visualized by the 3–4 PVU contour of the dynamical tropopause at 325 K potential temperature during the period between 18 and 23 February 1996 (Met Office analyses). The maps are stereographic projections with the Greenwich meridian at the bottom and the outer circle at 30N. Also shown is the vortex boundary (31, 38, and 44 PVU, heavy dotted lines) and temperature (188 K and 195 K, thick solid lines) in the lower stratosphere at the 475 K isentropic level (according to the Met Office analyses).

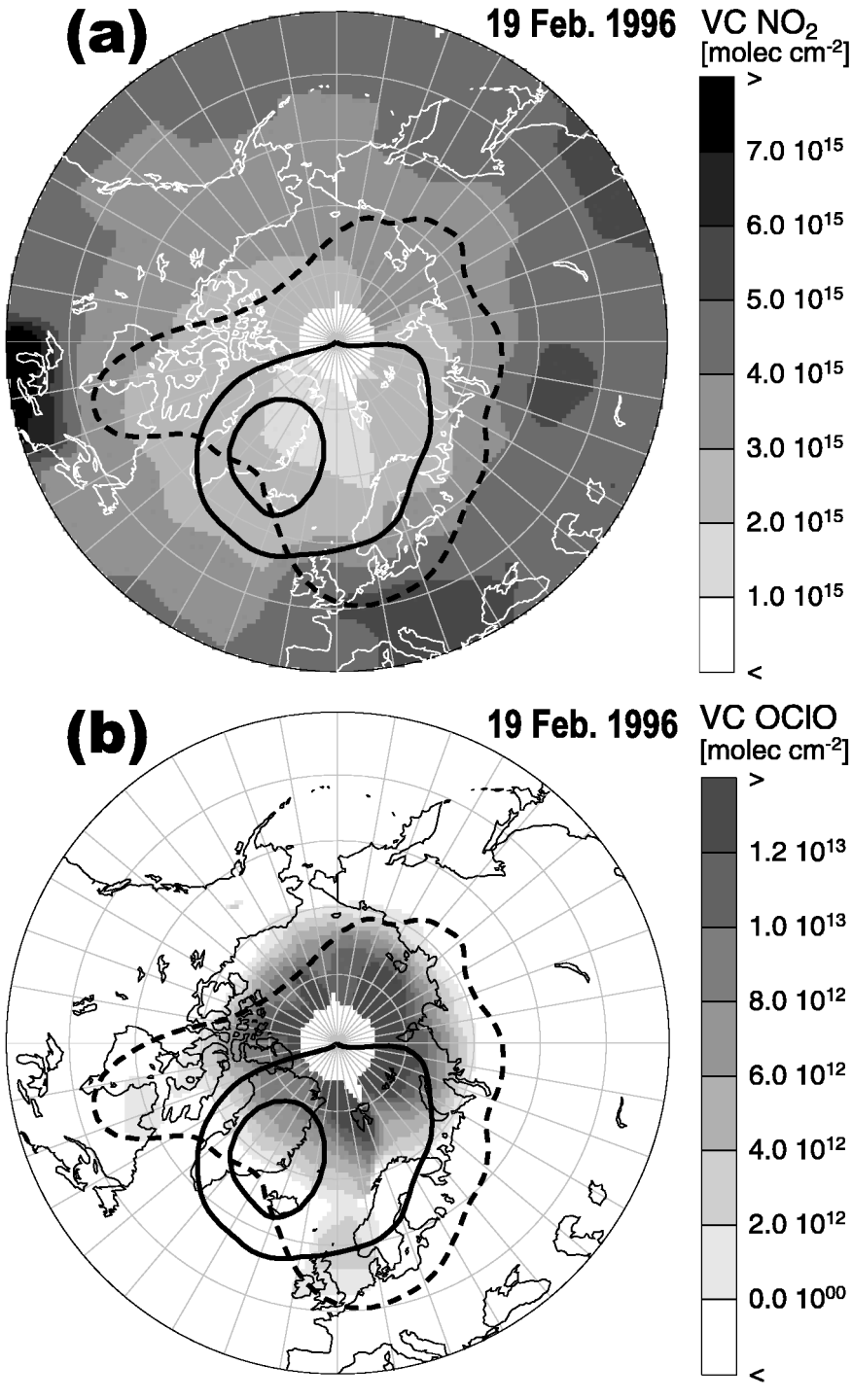

Figure 6. GOME vertical-column distributions of (a) NO_2, and (b) OClO in the northern hemisphere on 19 February. The thick dashed contour shows the 38 PVU isoline and the solid contours depict the 195 K (outer) and 188 K (inner) isotherms at the 475 K isentropic level, respectively.

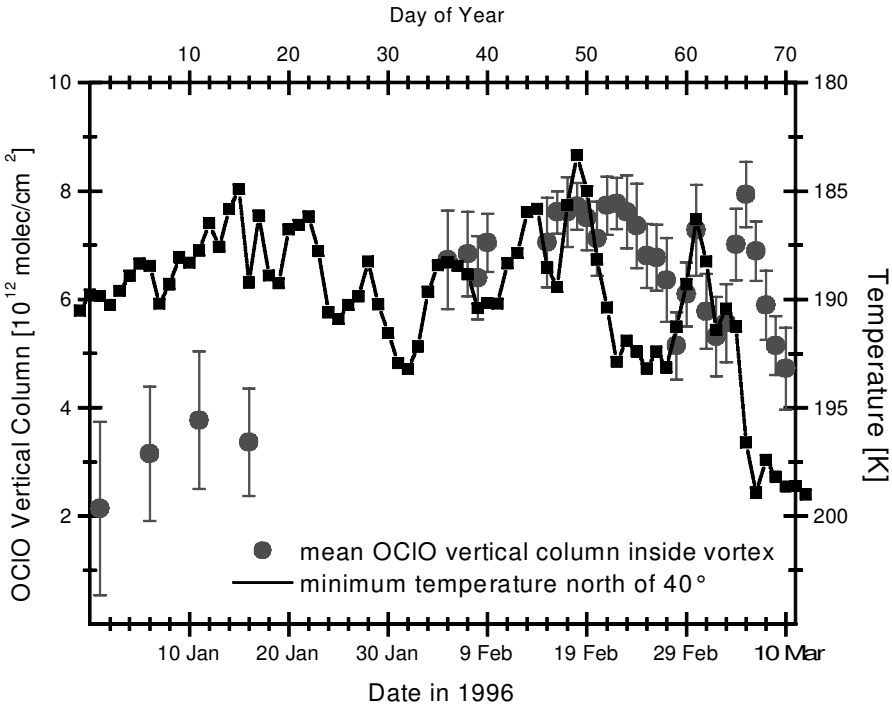

Figure 7. Time series of the vortex-averaged daily OClO total column from GOME between 86° and 90° solar zenith angle (grey circles) and minimum northern hemisphere temperature (square symbols) at the 475 K isentropic level (according to the European Centre for Medium-Range Weather Forecasts analyses). Error bars are standard deviations of the scattering around the daily OClO mean.

during PSC formation (Santee *et al.* 1996), and which explains the strong denoxification observed by GOME.

The OClO total-column distribution for the same day is also shown in Fig. 6. High OClO columns are observed throughout the polar vortex. The variability in the OClO columns is mainly due to variations of solar zenith angle (SZA) during GOME observations, which make interpretation of the OClO results difficult. In the troughs, where the PV contours extend further to the south (above eastern Canada and Europe), non-negligible OClO column amounts are observed at lower solar zenith angles, meaning that the region of large-scale chlorine activation almost encompasses the entire polar vortex. This is in agreement with elevated OClO amounts observed by a ground-based zenith-sky spectrometer in Bremen (Richter 1997). The question that arises is whether some additional chlorine activation has resulted from the strong stratospheric cooling at the tropospheric ridge. Figure 7 shows a time series of vortex-averaged daily OClO total columns observed in a SZA range of between 86° and 90°, an SZA range for which OClO columns are a maximum but still correlate linearly with the maximum daytime ClO and BrO (Sessler *et al.* 1995; Schiller and Wahner 1996). As the stratospheric temperature decreased below 188 K at the 475 K isentropic level after the middle of February, mean OClO columns exhibited a small increase of about 1×10^{12} molecules cm^{-2}, which is within the error of the GOME observations and, therefore, represents an insignificant change. A more significant OClO increase is, however, seen during the next mini-hole event in the first week of March after the OClO daily columns started to decrease from the February high values (see Fig. 7). This seems to suggest

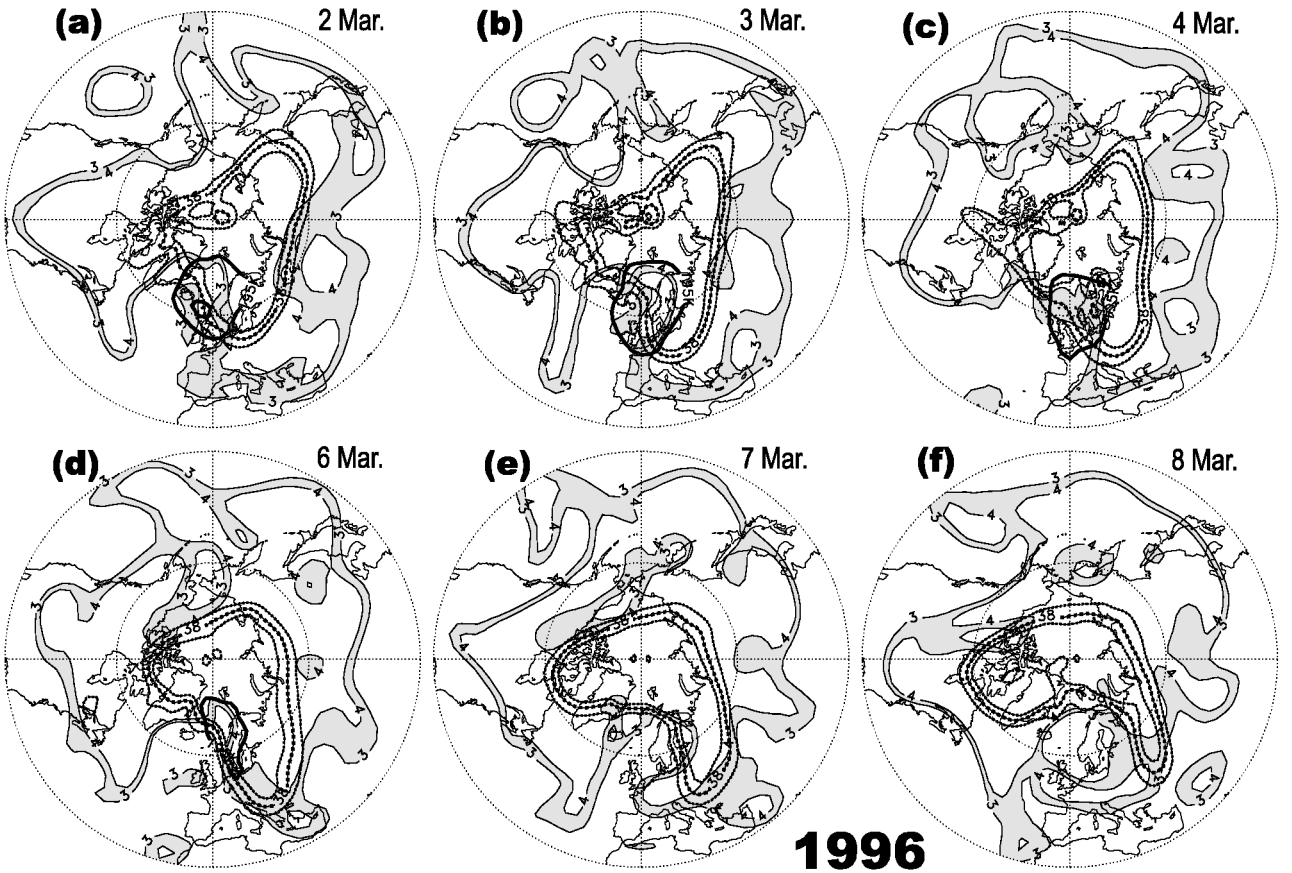

Figure 8. Rossby-wave breaking in the upper troposphere visualized by the 3–4 PVU contour of the dynamical tropopause on the 325 K isentropic surface during the period between 2 and 8 March 1996. The maps are stereographic projections with the Greenwich meridian at the bottom and the outer circle at 30°N. Also shown are the vortex boundary (31, 38, and 44 PVU, heavy dotted contours) and the temperature (185 and 195 K, thick solid lines) in the lower stratosphere at the 475 K isentropic level (according to the Met Office analyses).

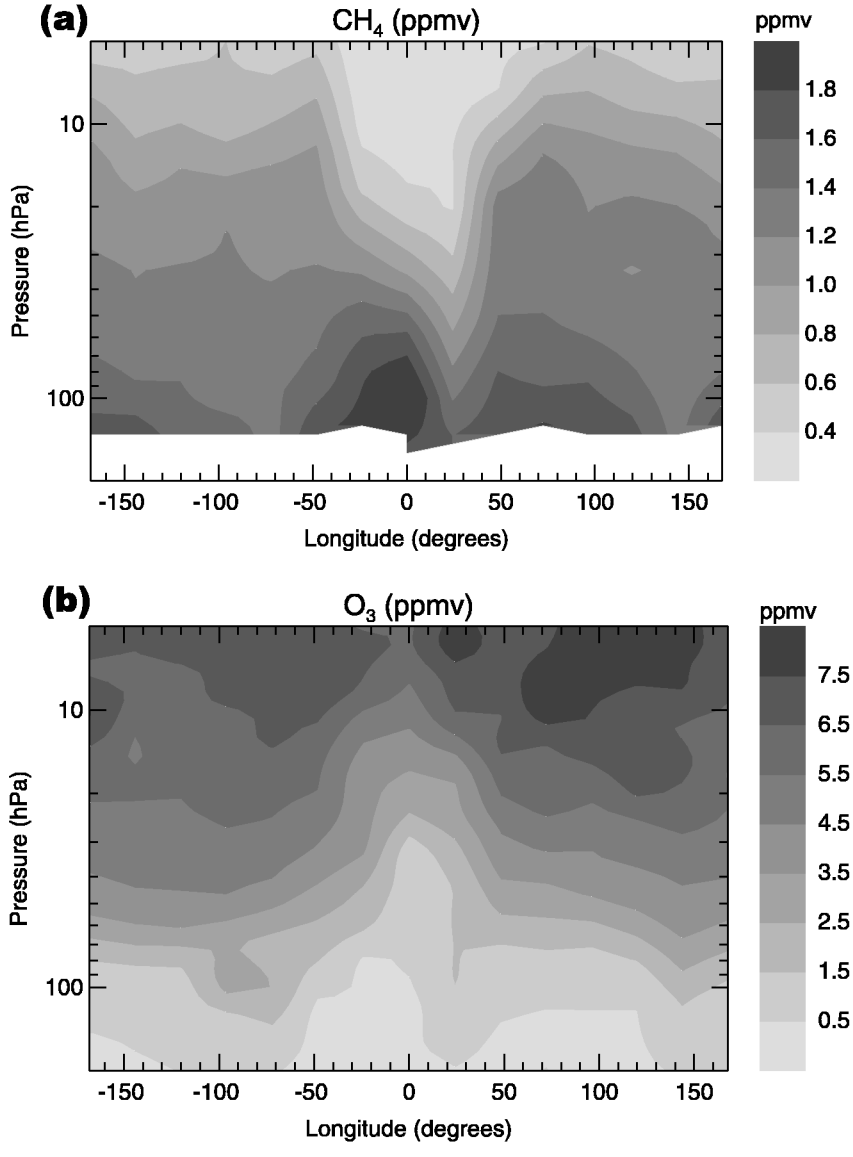

Figure 9. Zonal transects of HALOE observations of the (a) methane and (b) ozone mixing ratios at 52°N on 3 March 1996. The tangent points of the HALOE measurements contributing to the zonal transect are shown as dots in Fig. 4(b).

that, when the chlorine activation has reached its maximum level (full activation), as was apparently the case in February, additional increases in OClO columns are not observed despite a strong short-term reduction in lower-stratospheric temperatures during strong tropospheric ridging, whereas later in the year reactivation of chlorine can be observed.

Tropospheric wave activity related to the early March mini-hole sequence shown in Fig. 4 is displayed in Fig. 8. A region of very low stratospheric temperatures formed near the vortex edge above a tropospheric ridge centred north of Scotland (Figs. 8(a) and (b)). HALOE observations of strong aerosol extinction at 5 μm at 52°N confirm the existence of an extended PSC cloud centred at the Greenwich meridian during the

period between 2 March and 4 March (Müller *et al.* 1999). The zonal transect of HALOE measurements at 52°N on 3 March (Fig. 9) shows enhanced methane mixing ratios, with peak values of greater than about 1.8 ppmv* at 100 hPa inside the mini-hole, which is characteristic of lowermost stratospheric air masses being lifted by a high tropopause. The polar vortex is characterized by subsided air masses, i.e. by low methane mixing ratios of less than about 1 ppmv near 50 hPa. The dynamics of the tropospheric ridge moving beneath the vortex boundary region is illustrated by the large negative gradient of CH_4 mixing ratios between 100 and 20 hPa (vertically) and between 0°E and 30°W (horizontally). Low ozone mixing ratios in the lower stratosphere are indeed observed above the tropospheric ridge at 0°E.

In early March, low total-ozone values of below 250 DU were observed by GOME in this region between the British Isles, Iceland, and northern Scandinavia. From the MLS observations aboard UARS a reduced stratospheric ozone column (above 100 hPa) of 180–190 DU was reported (Manney *et al.* 1996a). The region of extremely low total ozone partly overlaps with the polar vortex, but also clearly extends outside the vortex edge, e.g., total ozone of less than 275 DU is observed south of Iceland at PV ≈20–25 PVU (Fig. 4). Under such circumstances, the relative effects of chemistry and dynamics on ozone are difficult to quantify.

5. Chemical ozone loss

Measurements of the vertical profile of the ozone mixing ratio on 3 March 1996 by HALOE allow further investigation of the cause of the observed low total-ozone values (see dots near the 50°N latitude circle in the corresponding GOME ozone plot of the same day in Fig. 4(b)). At 52°N comparable total-ozone values are observed at 24°W and 24°E; the observed ozone profiles, however, are very different (compare the solid triangle and solid diamond symbols in Fig. 10). Also shown in Fig. 10 are profiles of the proxy ozone, $\hat{O}_3$, expected in the absence of chemical removal of ozone.

The proxy-ozone volume mixing ratio was determined by expressing early vortex ozone concentrations in November as an empirical third-order polynomial function of the methane concentration for methane volume mixing ratios of between 0.5 ppmv and 1.6 ppmv (Müller *et al.* 1999). For a confined vortex air mass, this reference relationship is conserved over the course of the winter, if no chemical depletion occurs.

Chemical ozone loss will lead to a decrease of ozone values relative to the tracer values and thus leads to a modification of the reference relations. Mixing between different air masses may also lead to changes of the reference relation. Michelsen *et al.* (1998a, 1998b) and Plumb *et al.* (2000) suggested that mixing across the vortex edge of different air masses that lie on a nonlinear reference relationship leads to a change in ozone/tracer relationship which might be misinterpreted as chemical ozone loss. In contrast, Müller *et al.* (2002) argue that air outside the polar vortex is characterized by larger ozone values than the air inside, so that any mixing across the vortex edge should lead to an increase of ozone relative to a given tracer mixing ratio and, thus, to an underestimation of chemical ozone loss.

For the 1995/96 winter, however, it was shown that the correlation between long-lived tracers, here CH_4 and HF, remained constant throughout the vortex existence (Müller *et al.* 1999) and that the ozone/CH_4 relation did not change substantially between November and January (Müller *et al.* 1997a). It thus seems unlikely that mixing across the vortex edge did alter the ozone/methane correlation significantly over the

* Parts per million by volume.

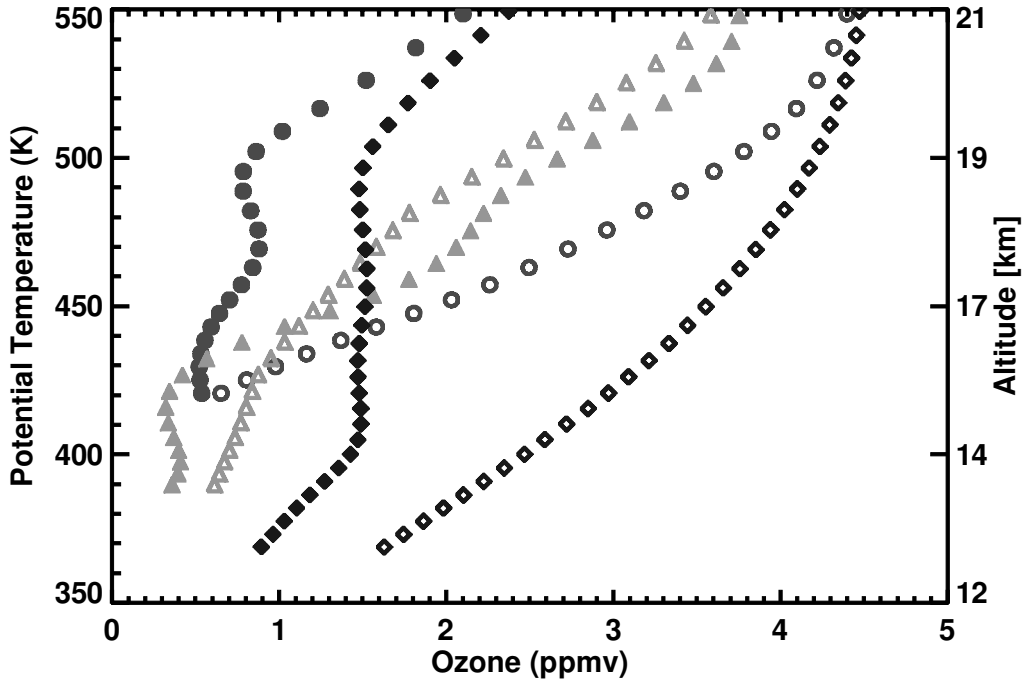

Figure 10. Vertical profiles of ozone mixing ratio measured by HALOE on 3 March 1996 at 52°N (solid symbols). Open symbols indicate the proxy ozone ($\hat{O}_3$) expected in the absence of chemistry. Observations at 24°W (triangles), 0°E (circles), and 24°E (diamonds) are shown.

TABLE 3. HALOE AND GOME OBSERVATIONS OF THE POTENTIAL VORTICITY AT THE 475 K ISENTROPIC LEVEL, THE TOTAL O_3, AND THE CALCULATED O_3 LOSS AT 52°N ON 3 MARCH 1996

Longitude	Potential vorticity (PVU)	O_3 (DU)	O_3 loss (DU)
−24°	27.8	281.0	3 ± 25
0°	32.4	263.3	60 ± 25
24°	48.4	348.7	136 ± 25

course of that winter. The deficit of ozone relative to the proxy ozone was thus assumed to be entirely due to accumulated chemical loss processes over the course of the winter. As the air masses outside the vortex in November are characterized by somewhat larger ozone mixing ratios than inside (Müller *et al.* 1999), the application of an early vortex relation as a reference for the profile at 24°W could lead to some underestimation of chemical ozone loss.

Integrating the deficit in ozone vertically yields the loss in column resulting from chemical depletion between November and early March (Table 3). Large chemical ozone loss is deduced at 24°E (inside the polar vortex) and practically no loss is detected at 24°W (outside the polar vortex), although the total-ozone columns are comparable in magnitude. It is concluded that the low total ozone at 24°W is caused by transport related to tropospheric subtropical-air intrusion (Fig. 8), while the low value at 24°E is mostly due to chemical loss. The ozone profile observed at 0°E at the edge of the polar vortex

shows a combination of both effects: chemical loss accumulated over the course of the winter and, at the same time, a dynamical reduction of the ozone column.

6. Discussion

Ozone mini-hole events are regular features in the polar region during the winter/spring season (Newman *et al.* 1988; McKenna *et al.* 1989; Petzoldt *et al.* 1994; Rabbe and Larsen 1992; James *et al.* 1997; James 1997, 1998; McCormack and Hood 1997). In February and March 1996 the mean positions of the vortex and, in particular, the cold centre were shifted towards the North Atlantic region (Fig. 2). The North Atlantic storm-track region, as defined by the maximum variability in the 500 mb geopotential height, is also the region where the largest variability in total ozone is generally observed (Orsolini *et al.* 1998). The extension of tropospheric ridges below the vortex edge region in late winter 1995/96 led to the particularly low lower-stratospheric temperatures above a high tropopause, and to extremely low Arctic total ozone. Such conditions were met because GOME made observations of minimum total-ozone values of 178 DU south of Greenland and close to the vortex edge on 19 February 1996 (see Fig. 3(c)). This was the lowest Arctic vortex ozone observed by GOME in any of the winters up to 1999/2000.

The low NO_2 and ozone total columns observed by GOME above the high tropopause region on 19 February confirm that the reduction in trace-gas concentrations in the lower stratosphere are mostly due to strong horizontal advection away from that region (Fig. 6(a)). The minimum NO_2 column region extended over a somewhat larger area than the ozone one did, which may be explained by the fact that the NO_2 concentration peaks at about 35 km. This means that advection in the lowermost stratosphere has a weaker influence on the column changes in NO_2 than on ozone which has its peak abundance in the lower stratosphere. The perturbation in the air-mass flow due to the tropospheric ridge, however, extends well into the middle stratosphere close to the 600 K isentropic level (about 24 km altitude), as seen in the negative relative PV (RPV) near 30°W in Fig. 11 (RPV is here defined as the modified PV (Lait 1994) referenced to 475 K potential temperature minus 38 PVU; therefore, positive values of RPV identify polar vortex air while large negative RPV values at the 325 K and 350 K isentropic levels indicate a high tropopause). This is also in accordance with the perturbation seen in the HALOE methane zonal transect in Fig. 9 reaching altitudes of about 30 km (10 hPa). The change in the NO_2 column because of horizontal advection at higher altitudes is, thus, plausible, but the denoxification as seen in Fig. 6(a) is not limited to the mini-hole region.

According to the Free University of Berlin meteorological analyses, temperatures above Greenland at the 30 hPa level were more than 15 K lower than the long-term values in February and 5 K lower in March 1996 (Naujokat *et al.*, personal communication). Despite the PSC I and II formation potential during these mini-hole events, the contribution to the chemical depletion over the timescale discussed here (a few days) is expected to be small because substantial ozone reduction through halogen-catalysed chemistry requires longer timescales (several weeks). During the early March mini-hole event, as shown in Figs. 4 and 8, an increase in the vortex-averaged OClO column correlates well with the drop in daily minimum lower-stratospheric temperature (Fig. 7). A secondary OClO maximum was reached the last day of that winter/spring season when stratospheric temperatures were below 195 K at the 475 K isentropic level on 6 March. The GOME data seem to suggest that dynamically induced additional chlorine activation is possible, but only if the active chlorine has decreased from its

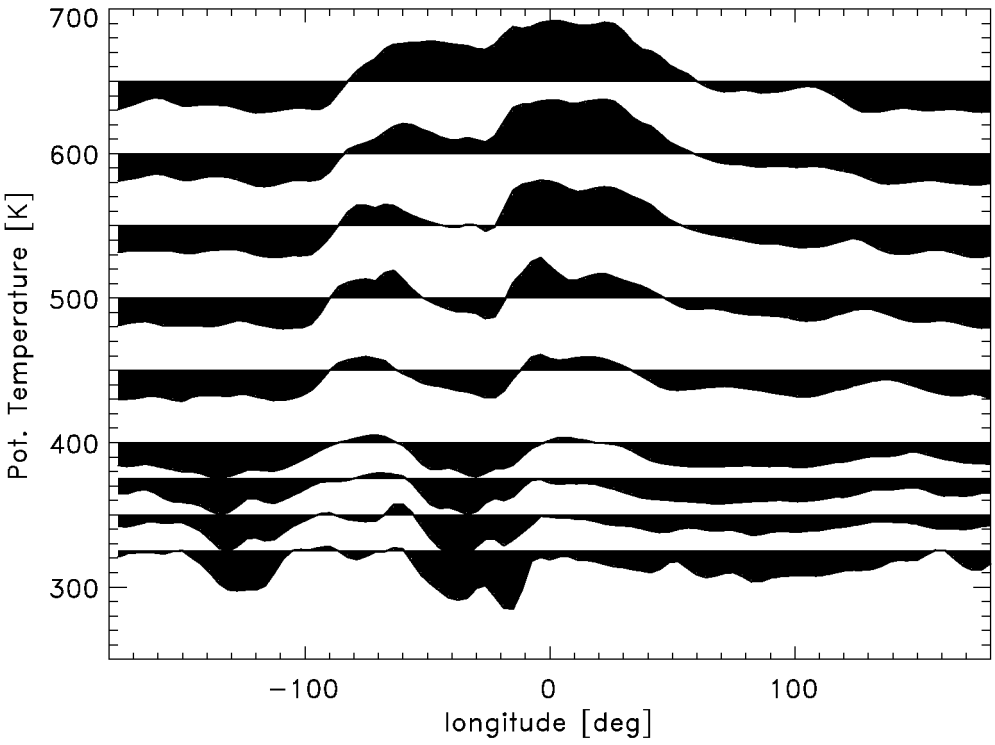

Figure 11. Zonal section (60°N) of relative potential vorticity (RPV) at isentropic levels 325, 350, 375, 400, 450, 500, 550, 600, and 650 K on 19 February 1996. The RPV is defined as the modified potential vorticity referenced to 475 K potential temperature minus 38 PVU (derived from the Met Office analyses). Positive RPVs indicate regions inside the vortex and the positions of the zero line of RPV are drawn at the corresponding levels. Large negative RPVs at the 325 K and 350 K isentropic levels are indicative of a high tropopause (30°W and 120°W). The perturbation of the polar vortex shape related to the tropospheric wave activity is visible up to 600 K (about 24 km altitude).

maximum concentration. Even though temperatures started to increase rapidly after 6 March, OClO levels showed a rather slow decrease in accordance with the continued chemical ozone losses observed until two weeks after the rise above the PSC formation temperature (Rex *et al.* 1997). Large-scale denitrification (due to sedimentation of PSC particles) removed the sources of NO_x, considerably slowing down the deactivation of active chlorine into $ClONO_2$.

Depending on the frequency and the duration of such mini-hole events (James 1998) additional chemical depletion, and subsequent enhanced chlorine activation induced by upper-tropospheric wave activity, may become significant (Grewe and Dameris 1997). It is possible that, in addition, mountain-induced gravity waves that are responsible for mesoscale PSC formation (generally not captured by the synoptic meteorological analyses as used in this study), also have a non-negligible contribution to the overall chemical ozone depletion owing to the fact that several high mountain ranges are distributed around the Arctic circle (Greenland, Scandinavia, and Ural mountains) (Carslaw *et al.* 1998). Nevertheless, it is more likely that, in warmer winters with rather sporadic PSC formation, the contribution of synoptic events in chemical ozone losses may become more significant.

From observations of total ozone alone it is difficult to distinguish unambiguously between chemically induced O_3 losses due to the presence of chlorine activation, and

dynamical decreases related to the meteorology, as shown in the comparison of chemical losses deduced from HALOE and the total-ozone observations by GOME (summarized in section 5 and Table 3).

7. Conclusion

The winter/spring 1995/96 was the first NH winter to be observed by GOME. Monthly-average total ozone amounts of about 335 DU inside the polar vortex were observed in February and March. These values are at a record low in the five-year GOME data record and lie about 110 DU below the long-term climatological mean. Indeed, severe chemical ozone loss in the polar vortex has been deduced by various methods (Manney *et al.* 1996a; Donovan*et al.* 1996; Rex *et al.* 1997 Müller *et al.* 1997a). In this study it was shown that, during the late winter period, upper-tropospheric wave activity below the polar vortex was intense and large excursions of subtropical air masses to very high latitudes (up to 80°N) were observed to have a strong impact on the shape of the lower-stratospheric polar vortex. Extremely low total-ozone columns, with values well below 250 DU, were observed by GOME at the vortex edge in localized regions above the North Atlantic and northern Europe during late February and March. These events have been shown to be ozone mini-hole events, which are associated with short-term and reversible dynamical reduction in ozone in a region of tropospheric ridging (high tropopause). In addition to extremely low ozone, very low lower-stratospheric temperatures, particularly over Greenland in late February and early March, were observed. These were sufficiently low for the occurrence of PSC II; indeed, some additional dynamically induced chlorine activation was observed in early March. The lifetime of an ozone mini-hole and the accompanying very cold region is of the order of a few days, and indicates that the major cause for the reduction of the ozone column to below 250 DU must be reversible transport processes. Depending on the frequency of occurrence of such events, the dynamically induced chlorine activation and subsequent chemical ozone loss may, however, become more significant. Enhanced OClO column amounts were, however, only observed in early March during that winter after the OClO column amounts observed by GOME started to decrease from the maximum level reached during the winter. In conclusion, the extremely low Arctic total-ozone values observed by GOME in late winter 1995/96 were caused by a superposition of chemical ozone loss accumulated over timescales of weeks and extreme short-term reversible dynamical reductions.

Acknowledgements

Part of this work was supported by the Bundesministerium für Bildung und Forschung via grant 01LO9607/1, by the University of Bremen, and by the State Bremen. We thank the German Remote Sensing Data Centre of the Deutsche Zentrum für Luft und Raumfahrt for providing the GOME operational level-2 data (total-ozone columns). The Met Office and the European Centre for Medium-Range Weather Forecasts are thanked for providing the meteorological datasets. We thank B. Naujokat for kindly providing the PSC statistics derived from the Free University of Berlin data. The support of the HALOE team at the National Aeronautics and Space Administration's Langley Research Center and of J. M. Russell III (HALOE Principal Investigator, Hampton University, USA) in providing the HALOE data is gratefully acknowledged. We thank the Atmospheric Chemistry Branch at the National Aeronautics and Space Administration's Goddard Space Flight Center for providing the TOMS/EP Version-7

data. Two anonymous reviewers are thanked for their valuable comments which helped improve this paper.

APPENDIX

Vortex boundary definition during the winter of 1995/96

The polar vortex boundary is characterized by maximum PV gradients and maximum westerly wind speeds (Nash *et al.* 1996; Rummukainen *et al.* 1994). The maximum PV gradient was determined by fitting a Gaussian to the first derivative of the PV as a function of equivalent latitude, as obtained from the ECMWF $2.5^\circ \times 2.5^\circ$ meteorological data. Between January and March 1996 the vortex edge at the 475 K isentropic level was, on average, at 37.7 ± 1.3 PVU. The average extent of the vortex edge region, as determined by the 1σ Gaussian width, was between 31.1 ± 2.3 PVU (outer edge) and 44.2 ± 2.1 PVU (inner edge). The error bounds calculated are 1σ deviations from the average of daily values over the course of the winter. In this paper, vortex boundary values of 31, 38, and 44 PVU at the 475 K isentropic level are adopted to describe the vortex boundary region during winter 1995/96. In other winters the vortex edge values may vary by 1–2 PVU from the 1996 values. This would only marginally affect the mean vortex total ozone as calculated in Table 1, where a vortex edge value of 38 PVU was assumed for all winters.

REFERENCES

Braathen, G. O., Rummukainen, M., Kyrö, E., Schmidt, U., Dahlback, A., Jørgensen, T. S., Fabian, R., Rudakov, V. V., Gil, M. and Borchers, R. 1994 Temporal development of of ozone within the Arctic vortex during the winter of 1991/92. *Geophys. Res. Lett.*, **21,** 1407–1410

Brühl, C., Drayson, S. R., Russell III, J. M., Crutzen, P. J., McInerney, J. M., Purcell, P. N., Claude, H., Gernandt, H., McGee, T. J., McDermid, I. S. and Gunson, M. R. 1996 Halogen Occultation Experiment ozone channel validation. *J. Geophys. Res.*, **101D,** 10217–10240

Burrows, J. P., Weber, M., Buchwitz, M., Rozanov, V., Ladstätter-Weißenmayer, A., Richter, A., DeBeek, R., Hoogen, R., Bramstedt, K., Eichmann, K.-U. and Eisinger, M. 1999 The Global Ozone Monitoring Experiment (GOME): Mission concept and first scientific results. *J. Atmos. Sci.*, **56,** 151–175

Carslaw, K. S., Wirth, M., Tsias, A., Luo, B. P., Dörnbrack, A., Leutbecher, M., Volkert, H., Renger, W., Bacmeister, J. T., Reimer, E. and Peter, Th. 1998 Increased stratospheric ozone depletion due to mountain-induced atmospheric waves. *Nature*, **391,** 675–678

Chipperfield, M. P. and Jones, R. L. 1999 Relative influences of atmospheric chemistry and transport on Arctic ozone trend. *Nature*, **400,** 551–554

Coy, L., Newman, P. A. and Nash, E. R. 1997 Meteorology of the polar vortex: Spring 1997. *Geophys. Res. Lett.*, **24,** 2693–2696

Cubashi, S. 1984 Preliminary results of ozone observations at Syowa stations from February 1982 to January 1983. *Mem. Nat. Polar Res. Special Issue, Jpn.*, **34,** 13–19

Donovan, D. P., Bird, J. C., Whiteway, J. A., Duck, T. J., Pal, S. R. and Carswell, A. I. 1995 Lidar observations of stratospheric ozone and aerosol above the Canadian high arctic during the 1994–95 winter. *Geophys. Res. Lett.*, **22,** 3489–3492

Donovan, D. P., Bird, J. C., Whiteway, J. A., Duck, T. J., Pal, S. R., Carswell, A. I., Sandilands, J. W. and Kaminski, J. W. 1996 Ozone and aerosol observed by lidar in the Canadian Arctic during the winter of 1995/1996. *Geophys. Res. Lett.*, **23,** 3317–3320

Donovan, D. P., Fast, H., Makino, Y., Bird, J. C., Carswell, A. I., Davies, J., Duck, T. J., Kaminski, J. W., McElroy, C. T., Mittermeier, R. L., Pal, S. R., Savastiouk, V., Velkov, D. and Whiteway, J. A. 1997 Ozone, column ClO, and PSC measurements made at the NDSC Eureka observatory (80°N, 86°W) during the spring of 1997. *Geophys. Res. Lett.*, **24,** 2709–2712

Farman, J. V., Gardiner, B. D. and Shanklin, J. D. 1985 Large losses of ozone in Antarctica reveal seasonal ClO_x/NO_x interaction. *Nature*, **315,** 207–210

Grewe, V. and Dameris, M. 1997 Heterogeneous PSC ozone loss during an ozone mini-hole. *Geophys. Res. Lett.*, **24,** 2503–2506

Hansen, G., Svenøe, T., Chipperfield, M., Dahlback, A. and Hoppe, U.-P. 1997 Evidence of substantial ozone depletion in winter 1996/97 over northern Norway. *Geophys. Res. Lett.*, **24,** 799–802

Herman, J. R., McPeters, R. and Larko, D. 1993 Ozone depletion at northern and southern latitudes derived from January 1979 to December 1991 Total Ozone Mapping Spectrometer data. *J. Geophys. Res.*, **98D,** 12783–12793

Hintsa, E. J., Newman, P. A., Jonsson, H. H., Webster, C. R., May, R. D., Herman, R. L., Lait, L. R., Schoeberl, M. R., Elkins, J. W., Wamsley, P. R., Dutton, G. S., Bui, T. P., Kohn, D. W. and Anderson, J. G 1998 Dehydration and denitrification in the Arctic polar vortex during the 1995–96 winter. *Geophys. Res. Lett.*, **25,** 501–504

Hoerling, M. P., Schaack, T. K. and Lenzen, A. J. 1991 Global objective tropopause analysis. *Mon. Weather Rev.*, **119,** 1816–1831

Hofmann, D., Deschler, T. L., Aimedieu, P., Matthews, W. A., Johnson, P. V., Kondo, Y., Sheldon, W. R., Byrne, E. L. and Benbrokke, J. R. 1989 Stratospheric clouds and ozone depletion in the Arctic during January 1989. *Nature*, **340,** 117–121

Hoskins, B. J., McIntyre, M. E. and Robertson, A. W. 1985 On the use and significance of isentropic potential vorticity maps. *Q. J. R. Meteorol. Soc.*, **111,** 877–946

James, P. M. 1997 An interhemispheric comparison of mini ozone-hole climatologies. *Geophys. Res. Lett.*, **25,** 301–304

1998 A climatology of ozone mini-holes over the northern hemisphere. *Int. J. Climatol.*, **18,** 1287–1303

James, P. M., Peters, D. and Greisiger, K. M. 1997 A study of ozone mini-hole formation using a tracer advection model driven by barotropic dynamics. *Meteorol. Atmos. Phys.*, **64,** 107–121

Knudsen, B. M., Larsen, N., Mikkelsen, I. S., Morcrette, J.-J., Braathen, G. O., Kyr, E., Fast, H., Gernandt, H., Kanzawa, H., Nakane, H., Dorokhov, V., Yushkov, V., Hansen, G., Gil, M. and Shearman, R. J. 1998 Ozone depletion in and below the Arctic vortex for 1997. *Geophys. Res. Lett.*, **25,** 627–630

Lait, L. R. 1994 An alternative form for potential vorticity. *J. Atmos. Sci.*, **51,** 1754–1759

Lambert, J.-L., van Roozendael, M., de Mazière, M. and Simon, P. C. 1999a Investigation of pole-to-pole performances of spaceborne atmospheric chemistry sensors with the NDSC *J. Atmos. Sci.*, **56,** 176–193

Lambert, J.-C., Peeters, P., Richter, A., Schutgens, N. A. J., Timofeyev, Y. M., Wagner, T., Burrows, J. P., Elansky, N. F., Elokhov, A. S., Gerard, P., Granville, J., Gruzdev, A. M., Ionov, D. V., Ionov, V. V., Koelemeijer, R. B. A., Ladstätter-Weißenmayer, A., Leue, C., Loyola, D., Platt, U., Postylyakov, O. V., Shalamiansky, A. M., Simon, P. C., Stammes, P., Thomas, W., van Roozendael, M., Wenig, M. and Wittrock, F. 1999b 'ERS-2 GOME data products delta characterization report 1999—Validation report for the GOME data processor upgrade: Level 0-to-1 Version 2.0 and Level 1-to-2 Version 2.7. Issue 0.1'. Unpublished report available at http://earth.esa.int/ gome_report99

Larsen N., Knudsen, B., Mikkelsen, I. S., Jørgensen, T. S. and Eriksen, P. 1994 Ozone depletion in the Arctic stratosphere in early 1993. *Geophys. Res. Lett.*, **21,** 1611–1614

Lin, J., Mohnen, V., Yue G., Atkinson, R. and Matthews, W. 1997 Intercomparison of stratospheric ozone profiles obtained by the Stratospheric Aerosol and Gas Experiment II, Halogen Occultation Experiment, and ozone sondes in 1994–1995. *J. Geophys. Res.*, **102D,** 16137–16144

Manney, G. L., Froidevaux, L., Waters, J. W., Elson, L. S., Fishbein, E. F. and Zurek, R. W. 1993 The evolution of ozone observed by UARS MLS in the 1992 late winter southern polar vortex. *Geophys. Res. Lett.*, **20,** 1279–1282

Manney, G. L., Froidevaux, L., Waters, J. W., Zurek, R. W., Read, W. G., Elson, L. S., Kumer, J. B., Mergenthaler, J. L., Roche, A. E., O'Neill, A., Harwood, R. S., Mackenzie, I. and Swinbank, R. 1994 Chemical depletion of ozone in the Arctic lower stratosphere during winter 1992–93. *Nature*, **370,** 429–434

Manney, G. L., Zurek, R. W., Froidevaux, L. and Waters, J. W. 1995 Evidence for Arctic ozone depletion in late February and early March 1994. *Geophys. Res. Lett.*, **22,** 2941–2944

Manney, G. L., Santee, M. L., Froidevaux, L., Waters, J. and Zurek, R. W. 1996a Polar vortex conditions during the 1995–96 Arctic winter: Meteorology and MLS ozone. *Geophys. Res. Lett.*, **23,** 3203–3206

Manney, G. L., Froidevaux, L., Waters, J. W., Santee, M. L., Read, W. G., Flower, D. A., Jarnot, R. F. and Zurek, R. W. 1996b Arctic ozone depletion observed by UARS MLS during the 1994–95 winter. *Geophys. Res. Lett.*, **23,** 85–88

Manney, G. L., Froidevaux, L., Santee, M. L., Zurek, R. W. and Waters, J. 1997 MLS observations of Arctic ozone loss in 1996–97. *Geophys. Res. Lett.*, **24,** 2697–2700

Manney, G. L., Lahoz, W. A., Swinbank R., O'Neill, A., Connew, P. M. and Zurek, R. W. 1999 Simulation of the December 1998 stratospheric major warming. *Geophys. Res. Lett.*, **26,** 2733–2736

McKenna, D. S., Jones. R. I., Austin, J., Browell, E. V., McCormick, M. P., Kreuger, A. J. and Tuck, A. F. 1989 Diagnostic studies of the Antarctic vortex during the 1987 Antarctic ozone experiment: Ozone mini-holes. *J. Geophys. Res.*, **94D,** 11641–11668

McCormack, J. P and Hood, L. L. 1997 The frequency and size of ozone 'mini-hole' events at northern midlatitudes in February. *Geophys. Res. Lett.*, **24,** 2647–2650

Michelsen, H. A., Manney, G. L., Gunson, M. R. and Zander, R. 1998a Correlations of stratospheric abundances of NO_y, O_3, N_2O, and CH_4 derived from ATMOS measurements. *J. Geophys. Res.*, **103D,** 28347–28360

1998b Correlations of stratospheric abundances of CH_4 and N_2O derived from ATMOS measurements. *Geophys. Res. Lett.*, **25,** 2777–2780

Müller, R., Crutzen, P. J., Grooß, J.-U., Brühl, C., Russell III, J. M. and Tuck, A. F. 1996 Chlorine activation and ozone depletion in the Arctic vortex: Observations by HALOE on UARS. *J. Geophys. Res.*, **101D,** 12531–12554

Müller, R., Crutzen, P. J., Grooß, J.-U, Brühl, C., Russell III, J. M., Gernandt, H., McKenna, D. S. and Tuck, A. F. 1997a Severe chemical ozone loss in the Arctic during the winter of 1995–96. *Nature*, **389,** 709–712

Müller, R., Grooß, J.-U., McKenna, D. S., Crutzen, P. J., Brühl, C., Russell III, J. M. and Tuck, A. F. 1997b HALOE observations of the vertical structure of chemical ozone depletion in the Arctic vortex during winter and early spring 1996–1997. *Geophys. Res. Lett.*, **24,** 2717–2720

Müller, R., Grooß, J.-U., McKenna, D. S., Crutzen, P. J., Brühl, C., Russell III, J. M., Gordley, L. L., Burrows, J. P. and Tuck, A. F. 1999 Chemical ozone loss in the Arctic vortex on the winter 1995–96: HALOE measurements in conjunction with other observations. *Ann. Geophys.*, **17,** 101–114

Müller, R., Schmidt, U., Engel, A., McKenna, D. S. and Proffitt, M. H. 2002 The O_3/N_2O relationship from balloon-borne observations as a measure of Arctic ozone loss in 1991–1992. *Q. J. R. Meteorol. Soc.*, in press.

Nash, E. R., Newman, P. A., Rosenfield, J. E. and Schoeberl, M. R. 1996 An objective determination of the polar vortex using Ertel's potential vorticity. *J. Geophys. Res.*, **101D,** 9471–9478

Naujokat, B. and Pawson S. 1996 The cold stratospheric winters 1994/1995 and 1995/1996. *Geophys. Res. Lett.*, **23,** 3703–3706

Newman, P. A., Lait, L. R., and Schoeberl, M. R. 1988 The morphology and meteorology of southern spring total ozone mini-holes. *Geophys. Res. Lett.*, **15,** 923–926

Newman, P. A., Gleason, J., McPeters, R. D. and Stolarski, R. S. 1997 Anomalously low ozone over the Arctic. *Geophys. Res. Lett.*, **24,** 2689–2692

O'Neill, A., Grose, W. L., Pope, V. D., Maclean, H. and Swinbank R. 1994 Evolution of the stratosphere during northern winter 1991/92 as diagnosed from U.K. Meteorological Office analyses. *J. Atmos. Sci.*, **51,** 2800–2817

Orsolini, Y. I., Stephenson, D. B. and Doblas-Reyes, F. J. 1998 Storm track signature in total ozone during northern hemisphere winter. *Geophys. Res. Lett.*, **25,** 2413–2416

Park, J. H., Russell III, J. M., Gordley, L. L., Drayson, S. R., Benner, D. C., McInerney, J. M., Gunson, M. R., Toon, G. C., Sen, B., Blavier, J.-F., Webster, C. R., Zipf, E. C., Erdman, P., Schmidt, U. and Schiller, C. 1996 Validation of Halogen Occultation Experiment CH_4 measurements from the UARS. *J. Geophys. Res.*, **101D,** 10183–10204

Pawson, S. and Naujokat, B. 1997 Trends in daily wintertime temperatures in the northern stratosphere. *Geophys. Res. Lett.*, **24,** 575–578

1999 The cold winters of the middle 1990s in the northern lower stratosphere. *J. Geophys. Res.*, **104D,** 14209–14222

Peter, T. 1997 Microphysics and heterogeneous chemistry of polar stratospheric clouds. *Ann. Rev. Phys. Chem.*, **48,** 785–822

Peters, D. and Waugh, D. W. 1996 Influence of barotropic shear on the poleward advection of upper-tropospheric air. *J. Atmos. Sci.*, **53,** 3013–3031

Petzoldt, K., Naujokat, B. and Neugebohren, K. 1994 Correlation between stratospheric temperature, total ozone, and tropospheric weather systems. *Geophys. Res. Lett.*, **21,** 1203–1206

Plumb, R. A., Waugh, D. W. and Chipperfield, M. P. 2000 The effects of mixing on tracer relationships in the polar vortices. *J. Geophys. Res.*, **105D,** 10047–10062

Proffitt, M. H., Margitan, J. A., Kelly, K. K., Loewenstein, M., Podolske, J. R. and Chan, K. R. 1990 Ozone loss inside the Arctic vortex inferred from high-altitude aircraft measurements. *Nature*, **347,** 31–36

Rabbe, A. and Larsen, S. H. H. 1992 Ozone mini-hole over Northern Scandinavia. *J. Atmos. Terrestr. Phys.*, **54,** 1447–1451

Rex, M., Harris, R. P., von der Gathen, P., Lehmann, R., Braathen, G. O., Reimer. E., Beck, A., Chipperfield, M. P., Alfier, R., Allaart, M., O'Connor, F., Dier, H., Dorokhov, V., Fast, H., Gil, M., Kyrö, E., Litynska, Z., Mikkelsen, I. S., Molyneux, M. G., Nakane, H., Notholt, J., Rummukainen, M., Viatta, P. and Wenger, J. 1997 Prolonged stratospheric ozone loss in the 1995–96 Arctic winter. *Nature*, **389,** 835–837

Rex, M., von der Gathen, P., Harris, N. R. P., Lucic, D., Knudsen, B. M., Braathen, G. O., Reid, S. J., de Backer, H., Claude, H., Fabian, R., Fast, H., Gil, M., Kyrö, E., Mikkelson, I. S., Rummukainen, M., Smit, H. G., Stähelin, J., Varotsos, C. and Zaitcev, I. 1998 In situ measurements of stratospheric ozone depletion rates in the Arctic winter 1991/92: A Lagrangian approach. *J. Geophys. Res.*, **103D,** 5843–5853

Richter, A. 1997 'Absorptionsspektroskopische Messungen stratosphärischer Spurengase über Bremen, 53°N'. PhD Thesis, University of Bremen, 1997

Richter, A., Wittrock, F., Eisinger, M. and Burrows, J. P. 1998 GOME observations of tropospheric BrO in Northern Hemispheric spring and summer 1997. *Geophys. Res. Lett.*, **25,** 2683–2686

Rozanov, V., Diebel, D., Spurr R. J. D. and Burrows, J. P. 1997 GOMETRAN: A radiative transfer model for the satellite project GOME—the plane parallel version. *J. Geophys. Res.*, **102,** 16683–16695

Rummukainen, M., Knudsen, B. and von der Gathen, P. 1994 Dynamical diagnostics of the edges of the polar vortices. *Ann. Geophys.*, **12,** 1114–1118

Russell III, J. M., Gordley, L. L., Park, J. H., Drayson, S. R., Hesketh, W. D., Cicerone, R. J., Tuck, A. F., Frederick, J. E., Harries, J. E. and Crutzen, P. J. 1993 The Halogen Occultation Experiment. *J. Geophys. Res.*, **98D,** 10777–10797

Santee, M. L., Manney, G. L., Read W. G., Froidevaux, L. and Waters, J. 1996 Polar vortex conditions during the 1995-96 Arctic winter: MLS ClO and HNO_3. *Geophys. Res. Lett.*, **23,** 3207–3210

Sessler, J., Chipperfield, M. P., Pyle, J. A. and Toumi, R. 1995 Stratospheric OClO measurements as a poor quantitative indicator of chlorine activation. *Geophys. Res. Lett.*, **22,** 687–690

Schiller, C. and Wahner, A. 1996 Comment on 'Stratospheric OClO measurements as a poor indicator of chlorine activation' by J. Sessler, M. P. Chipperfield, J. A. Pyle and R. Toumi. *Geophys. Res. Lett.*, **23,** 1053–1054

Schoeberl, M. R., Proffitt, M. H., Kelly, K. K., Lait, L. R., Newman, P. A., Rosenfield, J. E., Lowenstein, M., Podolske, J. R., Strahan, S. E. and Chan K. R. 1990 Stratospheric constituent trends from ER-2 profile data. *Geophys. Res. Lett.*, **17,** 469–427

Sinnhuber, B.-M., Langer, J., Klein, U., Raffalski, U., Künzi, K. and Schrems, O. 1998 Ground based millimeter-wave observations of Arctic ozone depletion during winter and spring 1996/97. *Geophys. Res. Lett.*, **25,** 3327–3330

Solomon, S. 1999 Stratospheric ozone depletion: A review of concepts and history. *Rev. Geophys.*, **37,** 275–316

Solomon, S., Garcia, R. R., Rowland, F. S. and Wuebbles, D. J. 1986 On the depletion of Antarctic ozone. *Nature*, **331,** 808–811

Swinbank, R. and O'Neill, A. 1994 A stratosphere-troposphere data assimilation system. *Mon. Weather Rev.*, **122,** 686–702

Von der Gathen, P., Rex, M., Harris, N. R. P., Lucic, D., Knudsen, B. M., Braathen, G. O., de Becker, H., Fabian, R., Fast, H., Gil, M., Kyrö, E., Mikkelsen, I. S., Rummukainen, M., Stähelin, J. and Vaotsos, C. 1995 Observational evidence for chemical ozone depletion over the Arctic in winter 1991–92. *Nature*, **375,** 131–134

Vömel, H., Rummukainen, M., Kivi, R., Karhu, J., Turunen, T., Kyrö, E., Rosen, J., Kjome, N. and Oltmans, S. 1997 Dehydration and sedimentation of ice particles in the Arctic stratospheric vortex. *Geophys. Res. Lett.*, **24,** 795–798

Waters, J. W., Froidevaux, L., Manney, G. L., Read, W. G. and Elson, L. S. 1993 MLS observations of lower stratospheric ClO and ozone in the 1992 southern hemisphere winter. *Geophys. Res. Lett.*, **20,** 1219–1222

Weber, M., Burrows, J. P. and Cebula, R. P. 1998 GOME solar UV/VIS irradiance measurements between 1995 and 1997—First results on proxy solar activity studies. *Solar Phys.*, **177,** 63–77

Wittrock, F., Richter, A. and Burrows, J. P. 1999 'Validation of GOME BrO and OClO observations in the Northern Hemisphere'. Pp. 735–738 in *European symposium on atmospheric measurements from space*. ESA Publication WP 161, European Space Agency, ISSN 1022-6656, Noordwijk, The Netherlands